New Phytologist

Research

# Terrestrial biosphere models may overestimate Arctic $CO_2$ assimilation if they do not account for decreased quantum yield and convexity at low temperature

**Alistair Rogers[1], Shawn P. Serbin[1], Kim S. Ely[1] and Stan D. Wullschleger[2]**

[1]Environmental and Climate Sciences Department, Brookhaven National Laboratory, Upton, NY 11973-5000, USA; [2]Environmental Sciences Division, Oak Ridge National Laboratory, Oak Ridge, TN 37831-6301, USA

Author for correspondence:
*Alistair Rogers*
*Tel: +1 631 344 2948*
*Email: arogers@bnl.gov*

Received: *9 November 2018*
Accepted: *10 February 2019*

*New Phytologist* (2019) **223:** 167–179
**doi**: 10.1111/nph.15750

**Key words:** absorptance, curvature, high latitude, light, photosynthesis, plant, tundra, vegetation.

## Summary

- How terrestrial biosphere models (TBMs) represent leaf photosynthesis and its sensitivity to temperature are two critical components of understanding and predicting the response of the Arctic carbon cycle to global change.
- We measured the effect of temperature on the response of photosynthesis to irradiance in six Arctic plant species and determined the quantum yield of $CO_2$ fixation ($\phi_{CO_2}$) and the convexity factor ($\theta$). We also determined leaf absorptance ($\alpha$) from measured reflectance to calculate $\phi_{CO_2}$ on an absorbed light basis ($\phi_{CO_2.a}$) and enabled comparison with nine TBMs.
- The mean $\phi_{CO_2.a}$ was 0.045 mol $CO_2$ $mol^{-1}$ absorbed quanta at 25°C and closely agreed with the mean TBM parameterisation (0.044), but as temperature decreased measured $\phi_{CO_2.a}$ diverged from TBMs. At 5°C measured $\phi_{CO_2.a}$ was markedly reduced (0.025) and 60% lower than TBM estimates. The $\theta$ also showed a significant reduction between 25°C and 5°C. At 5°C $\theta$ was 38% lower than the common model parameterisation of 0.7.
- These data show that TBMs are not accounting for observed reductions in $\phi_{CO_2.a}$ and $\theta$ that can occur at low temperature. Ignoring these reductions in $\phi_{CO_2.a}$ and $\theta$ could lead to a marked (45%) overestimation of $CO_2$ assimilation at subsaturating irradiance and low temperature.

## Introduction

Since the beginning of the last century atmospheric carbon dioxide concentration ($[CO_2]$) has risen by *c.* 100 μmol $mol^{-1}$ (33%), which has resulted in an average increase in the global annual near surface air temperature of *c.* 1°C. Over the same period, the temperature in the Arctic has increased by more than twice the global mean (USGCRP, 2017). Similarly, the annual amplitude of the seasonal cycle of $[CO_2]$ at high latitudes has increased approximately twice as much as the amplitude at lower latitudes (Keeling *et al.*, 1996; Graven *et al.*, 2013). This is widely considered to be due to enhanced productivity of high-latitude ecosystems, but the drivers and mechanism of the observed increase are still debated (Forkel *et al.*, 2016; Thomas *et al.*, 2016; Piao *et al.*, 2018). Therefore, the high sensitivity of the Arctic to climate change and the increasingly important, yet uncertain, role that Arctic ecosystems are playing in the global carbon cycle emphasises the need to advance the understanding and model representation of ecosystem processes and fluxes in the Arctic.

Photosynthesis responds, and acclimates, to both rising $[CO_2]$ and temperature (Ainsworth & Rogers, 2007; Yamori *et al.*, 2014; Dusenge *et al.*, 2019), and the response of photosynthesis to these two environmental drivers provides a partial explanation of the enhanced productivity at high latitudes. Currently, however, many terrestrial biosphere models (TBMs) markedly underestimate $CO_2$ assimilation in high latitude (Arctic and boreal) biomes (Graven *et al.*, 2013; Forkel *et al.*, 2016; Thomas *et al.*, 2016; Rogers *et al.*, 2017b; Piao *et al.*, 2018). An improved representation of photosynthesis in TBMs is key step toward reducing the model uncertainty associated with the carbon cycle at high latitudes, and increasing confidence in model projections of the response of high-latitude ecosystems to global change.

In most TBMs, leaf-level photosynthesis is represented by the model originally proposed by Farquhar, von Caemmerer and Berry (Farquhar *et al.*, 1980), hereafter the 'FvCB model'. In the simplest form of this model the rate of $CO_2$ assimilation ($A$, μmol $CO_2$ $m^{-2}$ $s^{-1}$) is determined by the minimum of the ribulose-1,5-bisphosphate(RuBP)-saturated $CO_2$ assimilation rate ($A_c$) and the RuBP-limited $CO_2$ assimilation rate ($A_j$, Eqn 1).

$$A = \min(A_c, A_j). \quad \text{Eqn 1}$$

$A_c$ and $A_j$ are determined as described by Eqns 2 and 3, where $V_{c,max}$ is the maximum rate of carboxylation (μmol $CO_2$ $m^{-2}$ $s^{-1}$), $C_i$ and $O_i$ are the intercellular $CO_2$ and $O_2$ concentrations (μmol $mol^{-1}$), $\Gamma^*$ is the $CO_2$ compensation point in the absence of nonphotorespiratory mitochondrial respiration in the light (μmol $mol^{-1}$), $K_c$ and $K_o$ are the

Michaelis–Menten coefficients of Rubisco activity for $CO_2$ and $O_2$, respectively (μM), and $R_d$ (μmol $CO_2$ $m^{-2}$ $s^{-1}$) is the daytime respiration rate that is not attributable to the photorespiratory pathway (von Caemmerer, 2000).

$$A_c = \frac{(C_i - \Gamma^*) V_{c,max}}{K_c\left(1 + \frac{O_i}{K_o}\right) + C_i} - R_d. \quad \text{Eqn 2}$$

$$A_j = \frac{(C_i - \Gamma^*) J}{4C_i + 8\Gamma^*} - R_d. \quad \text{Eqn 3}$$

The rate of electron transport ($J$, μmol electrons $m^{-2}$ $s^{-1}$) is dependent on the empirical relationship with incident irradiance ($I$, μmol quanta $m^{-2}$ $s^{-1}$). This relationship can be described by a nonrectangular hyperbola (shown solved for $J$ in Eqn 4). The initial slope of the response is determined by the maximum quantum yield of electron transport of absorbed light ($\phi_{ET.a}$, mol electrons $mol^{-1}$ absorbed quanta). The asymptote is determined by $J_{max}$, the maximum rate of electron transport. The empirical convexity, or curvature, factor (θ) determines the shape of the response curve and reflects the transition between $\phi_{ET.a}$ and $J_{max}$ where 1 represents an abrupt transition and 0 represents a long transition where both $\phi_{ET.a}$ and $J_{max}$ co-limit $J$ across a wide range of irradiance. The absorptance (α) is the fraction of incident visible light (*c.* 400–700nm) absorbed by the leaf.

$$J = \frac{I\alpha\phi_{ET.a} + J_{max} - \sqrt{(I\alpha\phi_{ET.a} + J_{max})^2 - 4\theta I\alpha\phi_{ET.a}J_{max}}}{2\theta}. \quad \text{Eqn 4}$$

The $\phi_{ET.a}$ can be further described by Eqn 5, where $f$ is the fraction of light absorbed by photosystem II (PSII) that is not used for photochemistry (von Caemmerer, 2000).

$$\phi_{ET.a} = \frac{1 - f}{2}. \quad \text{Eqn 5}$$

It has been repeatedly demonstrated that individual TBM implementation of the FvCB model and its parameterisation has a large influence on TBM outputs and yet there is considerable uncertainty and model divergence over the structure and parameterisation of these critical equations (Bonan *et al.*, 2011; Booth *et al.*, 2012; Lebauer *et al.*, 2013; Rogers, 2014; Sargsyan *et al.*, 2014; Rogers *et al.*, 2017a; Ricciuto *et al.*, 2018). The community is exploring a number of approaches that could enable improved parameterisation of the FvCB model. These efforts include measurement campaigns targeted at poorly represented biomes (e.g. Varhammar *et al.*, 2015; Rogers *et al.*, 2017b), the development of a number of approaches to map key photosynthetic parameters from remotely sensed data (Serbin *et al.*, 2015; Croft *et al.*, 2016; Alton, 2017), or approaches that link photosynthetic capacity to nutrient availability, or other abiotic drivers (Walker *et al.*, 2014; Ali *et al.*, 2015; Norby *et al.*, 2017; Smith *et al.*, 2019). With respect to high latitudes, some data on the key photosynthetic parameters $V_{c,max}$ and $J_{max}$, and their temperature responses, are now available for Arctic and boreal species (van de Weg *et al.*, 2013; Heskel *et al.*, 2014; Benomar *et al.*, 2017; Rogers *et al.*, 2017b; Schedlbauer *et al.*, 2018) addressing key uncertainties in Eqns 2 and 4. Here we continue our effort to advance model representation of photosynthesis in the high Arctic by focusing on model parameterisation associated with Eqn 4, that is the response of photosynthesis to irradiance. Specifically, we focus on the parameters α, ϕ and θ, which are assumed to be global constants in many TBMs. This addresses needs identified by the modeling community for an improved understanding of the limitations on photosynthesis at low temperature, and better understanding of global variation in ϕ (Dietze, 2014).

The maximum theoretical quantum yield of $CO_2$ assimilation ($\phi_{CO_2}$) for $C_3$ plants is 0.125, this means that 8 mol of quanta are required to fix 1 mol of $CO_2$. This estimate assumes full use of incident light for photochemistry (that is $\alpha = 1$ and $f = 0$, see Eqns 4 and 5), whole chain electron transport (no cyclic photophosphorylation), and exclusive use of NADPH for photosynthesis, and it ignores the potential requirement of amino acid biosynthesis, nitrate reduction and lipid metabolism for ATP and NADPH (von Caemmerer, 2000; Busch *et al.*, 2018). It is has been previously shown that there is very little variation in the maximum quantum yield of $CO_2$ assimilation of absorbed light ($\phi_{CO_2.a}$, mol $CO_2$ $mol^{-1}$ absorbed quanta) in $C_3$ species grown in nonstressful environments (Ehleringer & Bjorkman, 1977; Osborne & Garrett, 1983; Long *et al.*, 1993) where $\phi_{CO_2.a}$ measured in the absence of photorespiration varies little from the mean of 0.092 (Long *et al.*, 1993). However, reductions in ϕ and θ can occur in response to environmental conditions that decrease the potential for carbon assimilation, such as drought and low- or high-temperature stress (Bolharnordenkampf *et al.*, 1991; Groom & Baker, 1992; Ogren & Evans, 1992; Long *et al.*, 1994).

Light energy constantly damages the photosynthetic apparatus (Barber & Andersson, 1992; Takahashi & Murata, 2008). The D1 protein in the PSII reaction center is the primary target for photodamage and compromised D1 proteins are continually degraded and replaced in a costly repair cycle (Aro *et al.*, 1993; Murata & Nishiyama, 2018). As most plants encounter excess light conditions on a daily basis, they attempt to minimise photodamage through the regulated thermal dissipation of absorbed light, known as nonphotochemical quenching (NPQ) (Ort 2001). NPQ lowers the maximum quantum yield of PSII ($\phi_{PSII}$); this, in turn, results in a lower $\phi_{CO_2}$, but also a lower θ (Leverenz *et al.*, 1990; Long *et al.*, 1994; Zhu *et al.*, 2004). NPQ is beneficial in conditions of saturating light as it protects PSII without decreasing $A$. However, if NPQ remains engaged at low light the reductions in $\phi_{CO_2}$ and θ will limit $A$.

Low temperature exacerbates the effects of excess light, and leads to deeper reductions in both $\phi_{CO_2}$ and θ but also prolongs the effects of these reductions. Low temperature slows both the D1 repair cycle associated with recovery from photodamage, and the epoxidation of zeaxanthin associated with recovery from photoprotection (Bilger & Bjorkman, 1991; Barber & Andersson, 1992; Allakhverdiev & Murata, 2004; Takahashi &

Murata, 2008). However, in chilling tolerant or cold hardened plants, the reductions in $\phi_{CO_2}$ and θ are greatly reduced (Long *et al.*, 1994; Zhu *et al.*, 2004). Arctic plants grow at low temperatures but also experience excess irradiance regularly, suggesting that they could be susceptible to reductions in ϕ and θ caused by photoprotection or photodamage. In addition, the 24 h irradiance during the Arctic growth season may slow recovery from photoprotection or photodamage. Indeed, Arctic shrubs have been shown to have high xanthophyll cycle activity relative to other higher plants, suggesting acclimation or adaptation to excess light (Magney *et al.*, 2017). However, Arctic plants may also be well adapted to mitigate such reductions as they have evolved to grow at low temperature, and near-continuous light during the peak season. Furthermore, acclimation of photosynthesis to low growth temperatures should help to ensure high $A$ at low growth temperatures and therefore more effective utilisation of absorbed irradiance (Kumarathunge *et al.*, 2019). The current parameterisation of ϕ and θ in many TBMs assumes that these parameters are constant for all PFTs and insensitive to temperature, including Arctic vegetation (Dietze, 2014; Rogers *et al.*, 2017a). Furthermore, the theory and values used to parameterise current TBMs are based on unstressed temperate species. Here, we aimed to increase the understanding of photosynthesis in the Arctic, and provide new data and insights that could be used to advance the representation of high-latitude photosynthesis in TBMs. Our objective was to evaluate the current assumption in TBMs that Arctic species have high and temperature-insensitive values of ϕ and θ typical of unstressed plants, and to consider how that assumption might affect modeled leaf-level $CO_2$ assimilation.

## Materials and Methods

### Plant material

Measurements were made in 2016 on the coastal tundra at the Barrow Environmental Observatory (BEO), near Barrow, AK (71.3°N, 156.5°W; on 1 December 2016 Barrow was officially renamed Utqiaġvik). The landscape is characterised by ice-wedge polygons and thaw ponds, and has a low diversity of vascular plant species dominated by *Carex aquatilis* (Brown *et al.*, 1980). Mean annual air temperature is −12°C and mean annual precipitation is 106 mm, with the majority of precipitation falling as rain during the short summer. The soils are classified as Gelisols and are underlain by permafrost, with active-layer thickness ranging from 20 to 70 cm (Brown *et al.*, 1980; Bockheim *et al.*, 1999; Shiklomanov *et al.*, 2010).

Gas exchange and spectroscopy measurements were made over an area of *c.* 1 $km^2$ centered at 71.28°N, 156.65°W. This area is characterised by zones of significant permafrost degradation, standing water, dry high-centered polygons as well as relatively undisturbed low-centered polygonal ground that collectively provided a range of habitats for the different plant species of interest. Our goal was to measure the dominant vascular plants in this landscape but also cover a range of Arctic PFTs (Chapin *et al.*, 1996). In addition, our choice of species was constrained by the practical limitations of making gas exchange measurements. We studied six species covering four Arctic PFTs: grasses, *Arctagrostis latifolia* (R.Br.) Griseb, *Arctophila fulva* (Trin.) Andersson; sedges, *Carex aquatilis* Wahlenb., *Eriophorum angustifolium* Honck.; forbs, *Petasites frigidus* (L.) Fr.; and deciduous shrubs, *Salix pulchra* Cham. For each species we made measurements in a number of stands that were separated by geomorphological features to increase the likelihood that they were not members of the same clonal colony (Shaver *et al.*, 1979). Measurements were made over a 2-wk period in July 2016, beginning when the first mature leaves of these species were available for gas exchange, but before the onset of leaf senescence. Fig. 1 shows the ambient irradiance and air temperatures recorded during the period of our measurement campaign. All measurements were made on the most recent fully expanded mature leaves.

### Gas exchange and derived parameters

Gas exchange measurements were made *in situ* using five LI-6400XT gas exchange systems (Li-Cor, Lincoln, NE, USA) that were all recently calibrated (< 2 yr) and zeroed just before our measurement campaign using a common nitrogen standard (99.9998% nitrogen, $CO_2$ < 0.5 ppm, $H_2O$ < 0.5 ppm; Alphagaz 2, Air Liquide American Specialty Gases LLC, Anchorage, AK, USA). The differential between sample and reference infrared gas analyzers was maximised by using a 2 × 3 $cm^2$ leaf chamber equipped with a light-emitting diode (LED) red/blue light source (6400-02B LED light source; Li-Cor), and lowering the flow rate (typically to 350 μmol $s^{-1}$) until the $CO_2$ differential between the sample and reference chambers was at least 10 μmol $CO_2$ $mol^{-1}$. Flow rate was zeroed daily. We targeted two measurement temperatures of 5°C and 15°C. On a few occasions we were also able to make measurements at 25°C. These leaf temperatures were attained using the Peltier-based temperature control of the gas exchange system and by taking advantage of fluctuations in ambient temperature that occurred over the course of our field campaign (Fig. 1). The relative humidity of air entering the chamber was not controlled. Except for measurements made at 25°C, the leaf vapor pressure deficit was always below 1.0 kPa. After placing a leaf inside the leaf chamber, we checked for leaks by vigorously blowing through a tube directed at the edge of the gasket. When leaks were identified (fluctuations in $[CO_2]$ in the sample cell > 1 μmol $mol^{-1}$ over 15 s) the leaf was repositioned or leaks sealed with a silicone compound (Molykote 111, Dow Corning, MI, USA).

Following standard procedures (Long & Bernacchi, 2003; Bernacchi *et al.*, 2006), each leaf was first allowed to achieve steady-state $CO_2$ and water vapor exchange. During this equilibration period we controlled block temperature ($T_{block}$), reference chamber $[CO_2]$, and monitored the gradual increase in $A$ and stomatal conductance ($g_s$) until rates were constant and stable. At this point we switched temperature control from $T_{block}$ to $T_{leaf}$ and control of $[CO_2]$ from the reference to the sample chamber and set a $[CO_2]$ of 390 μmol $mol^{-1}$. Preliminary response curves indicated that full light saturation was not always attained below 1500 μmol quanta $m^{-2}$ $s^{-1}$. Furthermore, we observed that on

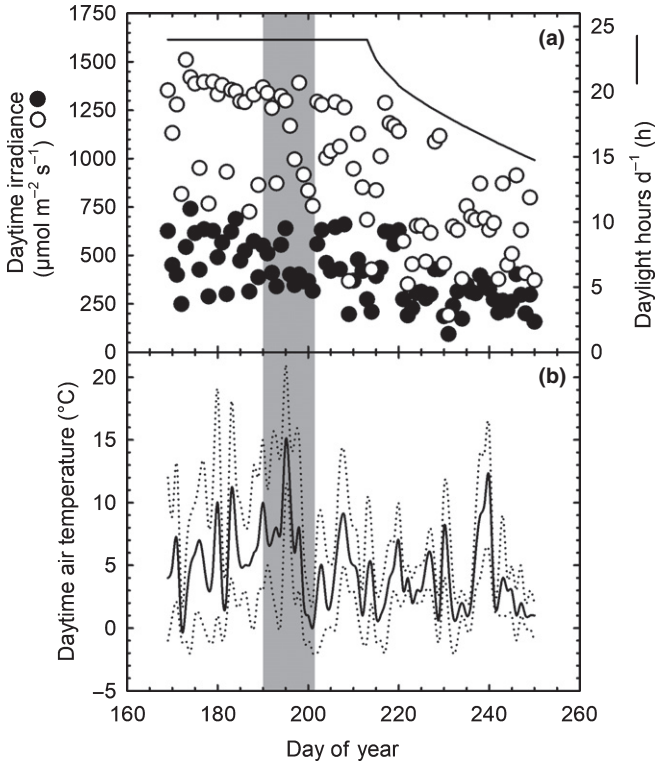


**Fig. 1** Irradiance and air temperature during the 2016 thaw season in Barrow (AK, USA). Mean (closed circles, a) and the 95$^{th}$ percentile (open circles, a) daily daytime irradiance (μmol m$^{-2}$ s$^{-1}$), total daylight h d$^{-1}$ (solid line, a) and mean (solid line, b) and minimum and maximum (dotted lines, b) daytime air temperature. Data were collected from a meteorological station located in the center of our field site that operated for most of the thaw season (Lewin *et al.*, 2016). The gray shaded area indicates the period when we conducted our measurements. Thaw season is defined as commencing on the first day of the first three consecutive days in the calendar year with an average temperature above freezing, and ending on the first day of the subsequent occurrence of 3 d with average temperatures below freezing.

cloud-free days the solar irradiance incident on the adaxial leaf surface of plants with largely erectophile leaf angle distributions could be > 2000 μmol m$^{-2}$ s$^{-1}$ due to the high solar zenith angle in the Arctic.

Each light-response curve consisted of 14 levels of irradiance (2000, 1500, 1250, 1000, 750, 500, 375, 200, 150, 100, 75, 50, 20 and 0 μmol m$^{-2}$ s$^{-1}$). Following an adjustment to each new irradiance, data were logged as soon as irradiance (SD < 1 μmol m$^{-2}$ s$^{-1}$ over 20 s), $T_{leaf}$ (SD < 0.2°C over 20 s), and $A$ (SD < 0.2 μmol m$^{-2}$ s$^{-1}$ over 20 s) were stable. When the leaf did not fill the leaf chamber, the enclosed leaf area was estimated as described previously (Rogers *et al.*, 2017b) and data recalculated using measured leaf area. Note that while we did measure $A$ in the darkness as part of our light-response protocol, this measurement was not preceded by a sufficient dark adaptation period to provide a reliable estimate of $R_{dark}$, was not used in our analysis and is not reported.

This protocol enabled us to measure the response of $A$ to irradiance while maintaining control of leaf temperature and the $CO_2$ concentration surrounding the leaf despite the wide range in incident light and $A$ that occurred over the course of the measurement. Supporting Information Fig. S1 shows examples of raw gas exchange data for two species, *P. frigidus*, a broad-leaved forb where the leaf filled the sample chamber and *A. latifolia*, a graminoid, where the leaf partially filled the sample chamber, measured at 5°C, 15°C and 25°C.

A nonrectangular hyperbola (Eqn 6) was fit to the resulting photosynthetic light-response curves using a two-step process whereby we first fitted the initial slope of the response curve (Posada *et al.*, 2009), where $\phi_{CO_2.i}$ is the maximum quantum yield of $CO_2$ assimilation of incident light (mol $CO_2$ mol$^{-1}$ incident quanta) and $A_{sat.g}$ is the light saturated gross photosynthetic rate (μmol m$^{-2}$ s$^{-1}$).

$$A = \frac{I\phi_{CO_2.i}A_{sat.g} - \sqrt{(I\phi_{CO_2.i} + A_{sat.g})^2 - 4\theta I\phi_{CO_2.i}A_{sat.g}}}{2\theta} - R_d. \quad \text{Eqn 6}$$

After examination of our dataset we elected to omit data collected below an irradiance of 20 μmol mol$^{-1}$ and above an irradiance 100 μmol mol$^{-1}$ to minimise the potential overestimation of the initial slope ($\phi_{CO_2.i}$) due to the influence of the Kok effect, and to limit potential underestimation of $\phi_{CO_2.i}$ by including points from the transition zone (Singsaas *et al.*, 2001; Farquhar & Busch, 2017). In addition, after examination of individual curves we further restricted maximum irradiance to 75 μmol mol$^{-1}$ in several cases to ensure that the portion of the curve used to derive $\phi_{CO_2.i}$ was strictly light limited. For each curve, the derived $\phi_{CO_2.i}$ was then fixed in Eqn 6 and used to derive the remaining parameters. As the initial slope of the response curve was fitted to data above a potential Kok kink, the derived $R_d$ could also be considered to be equal to $R_{light}$, but note the current debate over this issue (Buckley *et al.*, 2017; Farquhar & Busch, 2017; Tcherkez *et al.*, 2017). Our estimates of $R_d$ were not corrected for changes in $C_i$ (Kirschbaum & Farquhar, 1987). The code used to fit our measurements and derive parameters can be found on GitHub (https://github.com/TESTgroup-BNL/Rogers_etal_NGEEArctic_LightResponse).

## Absorptance

We measured leaf-level reflectance on each sample leaf using a portable, full range (that is 0.35–2.5 μm) spectroradiometer together with a leaf clip assembly with an internal, calibrated light source (HR-1024i; Spectra Vista Corporation, Poughkeepie, NY, USA). Each measurement was referenced against a standard (Spectralon®; LabSphere, Inc., North Sutton, NH, USA) to calculate leaf reflectance from the ratio of target and standard calibrated radiance measurements for each leaf. We collected two to five measurements over the adaxial surface of each leaf to calculate an average, depending on the leaf size and morphology. Spectral discontinuities in the detector overlap areas were corrected using the SVC instrument software before sample averaging and other quality control steps, as described previously (Serbin *et al.*, 2014) using the R-

FieldSpectra package (https://github.com/serbinsh/R-FieldSpectra). We then calculated leaf spectral absorptance using the measured leaf reflectance as described previously (Shiklomanov *et al.*, 2016; Wu *et al.*, 2018). The code used to invert the leaf reflectance observations to derive leaf absorptance, input observations and example output can be found on GitHub (https://github.com/TESTgroup-BNL/Rogers_etal_NGEEArctic_LightResponse).

### Models considered

For comparison with TBM formulations used to represent the leaf-level response of photosynthesis to irradiance we considered the models represented in the fourth and fifth phases of the Coupled Climate-Carbon Cycle Model Intercomparison Project (Friedlingstein *et al.*, 2006, 2014) and those identified in a review of global-scale models (Smith & Dukes, 2013). As recently highlighted (Rogers *et al.*, 2017a), TBMs have considerable variation in their underlying assumptions about leaf and canopy photosynthesis, as do the models considered here (Table 1). In this study we focused on TBM formulations associated with the leaf-level response of photosynthesis to irradiance. To enable comparison of our measurements of $\phi_{CO_2.i}$ with TBM model assumptions, where $\alpha$ varied among TBMs, we calculated the quantum yield of $CO_2$ fixation on an absorbed light basis ($\phi_{CO_2.a}$) using Eqn 7 (von Caemmerer, 2000), where $C_i$ is the average low light (< 100 μmol quanta $m^{-2}$ $s^{-1}$) intercellular [$CO_2$] from our measurements (5°C, 363 μmol $CO_2$ $mol^{-1}$; 15°C, 330 μmol $CO_2$ $mol^{-1}$; 25°C, 303 μmol $CO_2$ $mol^{-1}$; the $C_i$ at 10°C and 20°C was interpolated from these three points).

$$\phi_{CO_2.a} = \frac{(C_i - \Gamma^*)}{(8C_i + 16\Gamma^*)}(1-f)\alpha. \quad \text{Eqn 7}$$

Eqns 8 (BETHY, CLM4.5, G'DAY, Orchidee), 9 (CanESM, JULES) and 10 (ED2, IBIS, LM3) were used to scale $\Gamma^*$ from the model reference temperature ($T_{ref}$) to the measured $T_{leaf}$ using model specific parameters, kinetic constants and temperature response functions ($E_a$ and $Q_{10}$, Table 1) as described previously (Collatz *et al.*, 1991; Foley *et al.*, 1996; Oleson *et al.*, 2013), where $\tau_{ref}$, is the $CO_2 : O_2$ specificity ratio at $T_{ref}$, $O_i$ was assumed to be 210 mmol $mol^{-1}$ and $R$ is the universal gas constant (8.314 J $mol^{-1}$ $K^{-1}$).

$$\Gamma^*_{T_{leaf}} = \Gamma^*_{T_{ref}} \exp\left[\frac{E_a(T_{leaf} - T_{ref})}{(T_{ref} R T_{leaf})}\right]. \quad \text{Eqn 8}$$

$$\Gamma^*_{T_{leaf}} = \frac{O_i}{2\left(\tau_{T_{ref}} Q_{10}^{\left(\frac{T_{leaf}-T_{ref}}{10}\right)}\right)}. \quad \text{Eqn 9}$$

$$\Gamma^*_{T_{leaf}} = \frac{O_i}{2\left(\tau_{T_{ref}} \exp^{E_a\left(\frac{1}{T_{ref}-273.15} - \frac{1}{T_{leaf}-273.15}\right)}\right)}. \quad \text{Eqn 10}$$

### Statistical analysis

Due to our inability to collect data at all temperatures in all species, and loss of some replication following initial data quality assessment, the final replication was uneven (Table 2). Spectral measurements were made on all leaves upon which we attempted to make gas exchange measurements and included some additional measurements that were not associated with gas exchange. A two-way analysis of variance (ANOVA) was used to identify significant effects of species and temperature associated with the data in Table 2. Note that due to poor replication of the serendipitous data collection at 25°C; the data from 25°C were not included in the statistical analysis of species effects. However, we felt that it was important to consider the data collected at 25°C because of the scarcity of 25°C measurements in Arctic vegetation, and because their inclusion allowed a direct comparison to TBM assumptions at the common reference temperature without the need for extrapolation. A one-way ANOVA was used to identify significant differences in absorptance among species. The effect of temperature on the pooled species data (collected at 5°C, 15°C and 25°C) was assessed with a one-way ANOVA. For a given temperature, two sample and one-sample *t*-tests were used to compare model assumptions to observations.

### Data availability

To allow for future reanalysis and synthesis of our data, and to maximise further use of it by the modeling community, all our data – including our raw gas exchange data – are available online (Rogers *et al.*, 2019; Serbin, 2019).

## Results

### Measured response of photosynthesis to irradiance

Table 2 shows the mean values for parameters derived from individual photosynthetic light-response curves measured in six Arctic species at 5°C and 15°C. Fig. 2 shows synthetic light-response curves plotted using the mean parameters presented in Table 2. There was significant variation among species in $\phi_{CO_2.i}$ ($F_{5,100} = 3.3$, $P < 0.01$), but not θ ($F_{5,100} = 1.7$, $P = 0.13$), $A_{sat.g}$ ($F_{5,100} = 1.0$, $P = 0.45$) or $R_d$ ($F_{5,100} = 1.1$, $P = 0.38$) and a significant effect of leaf temperature on all parameters ($\phi_{CO_2.i}$, $F_{1,100} = 83$, $P < 0.001$; $A_{sat.g}$ $F_{1,100} = 158$, $P < 0.001$; $R_d$, $F_{1,100} = 30$, $P < 0.001$) except θ where the effect was only marginally significant ($F_{1,100} = 3.4$, $P = 0.07$). There was a significant species × temperature interaction for $\phi_{CO_2.i}$ ($F_{5,100} = 2.7$, $P < 0.05$) and $A_{sat.g}$

**Table 1** Terrestrial biosphere model (TBM) parameterisation associated with the response of photosynthesis to irradiance.

| TBM | α | *f* | $T_{ref}$ (°C) | $\Gamma^*_{ref}$ (μmol mol$^{-1}$) | $\tau_{ref}$ | $E_a$ Γ* (kJ mol$^{-1}$) | $E_a$ τ | $Q_{10}$ τ | $\phi_{CO_2.i.25}$ (mol $CO_2$ mol$^{-1}$ incident quanta) | $\phi_{CO_2.a.25}$ (mol $CO_2$ mol$^{-1}$ absorbed quanta) |
|---|---|---|---|---|---|---|---|---|---|---|
| BETHY | 0.88 | 0.44 | 25 | 42.75 | na | 37.83 | na | na | 0.047 | 0.041 |
| CanESM | 0.85 | 0.36 | 25 | na | 2600 | na | na | 0.57 | 0.055 | 0.047 |
| CLM4.5 | 0.85 | 0.15 | 25 | 42.75 | na | 37.83 | na | na | 0.071 | 0.060 |
| ED2 | 0.73 | 0.36 | 15 | na | 4500 | na | −5000 | na | 0.050 | 0.036 |
| G'DAY | 0.85 | 0.48 | 25 | 42.75 | na | 37.83 | na | na | 0.044 | 0.037 |
| IBIS | 0.86 | 0.36 | 15 | na | 4500 | na | −5000 | na | 0.050 | 0.043 |
| JULES | 0.85 | 0.36 | 25 | na | 2600 | na | na | 0.57 | 0.055 | 0.047 |
| LM3 | 0.85 | 0.52 | 15 | na | 4500 | na | −5000 | na | 0.037 | 0.032 |
| Orchidee | 0.84 | 0.26 | 25 | 42.75 | na | 37.83 | na | na | 0.062 | 0.052 |

The leaf absorptance (α), the fraction of light not used for photosynthesis (*f*), the model reference temperature ($T_{ref}$), the $CO_2$ compensation point in the absence of mitochondrial respiration in the light at $T_{ref}$ ($\Gamma^*_{ref}$), the $CO_2$ : $O_2$ specificity ratio at $T_{ref}$ ($\tau_{ref}$), temperature response parameters used to scale Γ* and τ ($E_a$ Γ*, $E_a$ τ, and $Q_{10}$ τ). The quantum yield of $CO_2$ assimilation of incident irradiance ($\phi_{CO_2.i}$) at 25°C was calculated using Eqns 8–10 using measured intercellular $CO_2$ concentration, intercellular $O_2$ concentration = 210 mmol mol$^{-1}$ and $R$ = 8.314 J mol$^{-1}$ K$^{-1}$. The quantum yield of $CO_2$ assimilation of absorbed irradiance ($\phi_{CO_2.a}$) at 25°C was calculated using Eqn 7, na, not applicable. TBM model abbreviations and key model references are: BETHY, Biosphere Energy Transfer Hydrology scheme (Ziehn *et al.*, 2011); CTEM, Canadian Terrestrial Ecosystem Model (Melton & Arora, 2016) CLM4.5, the Community Land Model v.4.5 (Oleson *et al.*, 2013); ED2, Ecosystem Demography model v.2 (Medvigy *et al.*, 2009); G'DAY, Generic Decomposition and Yield model (M. Jiang *et al.*, unpublished; Medlyn *et al.*, 2000); IBIS, Integrated Biosphere Simulator (Foley *et al.*, 1996); JULES, Joint UK Land Environment Simulator (Harper *et al.*, 2016); LM3, Geophysics Fluid Dynamics Laboratory Land Model v.3; Orchidee, Organizing Carbon and Hydrology in Dynamic Ecosystems model (Yin & Struik, 2009).

**Table 2** Parameters fitted from the leaf-level response of photosynthesis to incident irradiance.

| $T_{leaf}$ (°C) | Species (*n*) | $\phi_{CO_2.i}$ (mol $CO_2$ mol$^{-1}$ quanta) | $A_{sat.g}$ (μmol m$^{-2}$ s$^{-1}$) | θ (dimensionless) | $R_d$ (μmol m$^{-2}$ s$^{-1}$) |
|---|---|---|---|---|---|
| 5.0 ± 0.11 | *A. latifolia* (11) | 0.028 ± 0.002 | 11.0 ± 0.8 | 0.42 ± 0.08 | 1.12 ± 0.2 |
| 4.8 ± 0.09 | *A. fulva* (9) | 0.029 ± 0.002 | 11.9 ± 1.1 | 0.51 ± 0.06 | 1.61 ± 0.3 |
| 4.9 ± 0.03 | *C. aquatilis* (6) | 0.025 ± 0.004 | 9.9 ± 1.0 | 0.27 ± 0.07 | 1.72 ± 0.3 |
| 5.0 ± 0.10 | *E. angustifolium* (8) | 0.028 ± 0.004 | 13.3 ± 0.6 | 0.34 ± 0.09 | 1.73 ± 0.4 |
| 5.0 ± 0. 05 | *P. frigidus* (5) | 0.028 ± 0.003 | 12.5 ± 1.3 | 0.37 ± 0.06 | 1.77 ± 0.3 |
| 4.9 ± 0.02 | *S. pulchra* (11) | 0.031 ± 0.002 | 10.2 ± 0.9 | 0.59 ± 0.06 | 0.98 ± 0.2 |
| 14.9 ± 0.02 | *A. latifolia* (10) | 0.034 ± 0.002 | 18.2 ± 0.7 | 0.43 ± 0.08 | 2.31 ± 0.3 |
| 14.9 ± 0.01 | *A. fulva* (14) | 0.046 ± 0.002 | 19.3 ± 1.2 | 0.51 ± 0.06 | 2.00 ± 0.2 |
| 14.9 ± 0.01 | *C. aquatilis* (6) | 0.039 ± 0.002 | 22.7 ± 1.0 | 0.38 ± 0.03 | 2.67 ± 0.4 |
| 14.9 ± 0.02 | *E. angustifolium* (11) | 0.037 ± 0.002 | 18.9 ± 1.1 | 0.52 ± 0.07 | 2.12 ± 0.2 |
| 14.9 ± 0.03 | *P. frigidus* (10) | 0.051 ± 0.003 | 16.2 ± 1.1 | 0.60 ± 0.04 | 2.82 ± 0.2 |
| 14.9 ± 0.02 | *S. pulchra* (11) | 0.042 ± 0.002 | 20.5 ± 1.0 | 0.56 ± 0.07 | 2.45 ± 0.2 |
| 24.9 ± 0.03 | *A. latifolia* (4) | 0.043 ± 0.003 | 18.5 ± 1.0 | 0.67 ± 0.04 | 2.45 ± 0.3 |
| n.d | *A. fulva* | nd | nd | nd | nd |
| 24.8 ± 0.13 | *C. aquatilis* (3) | 0.056 ± 0.013 | 14.1 ± 3.1 | 0.56 ± 0.05 | 1.61 ± 0.6 |
| 24.8 | *E. angustifolium* (1) | 0.042 | 14.2 | 0.72 | 2.22 |
| 24.9 ± 0.01 | *P. frigidus* (5) | 0.055 ± 0.002 | 16.5 ± 0.8 | 0.71 ± 0.03 | 3.32 ± 0.42 |
| n.d. | *S. pulchra* | nd | nd | nd | nd |

Measurements were made *in situ* at three target leaf temperatures for six species growing on the Barrow Environmental Observatory, Barrow, AK. The quantum yield of $CO_2$ fixation based on incident irradiance ($\phi_{CO_2.i}$), light saturated gross $CO_2$ assimilation rate ($A_{sat.g}$), the curvature factor (θ), and the daytime respiration rate ($R_d$). Parameters were derived by fitting Eqn 6 to individual light-response curves. Data are means ± SEM. For a given measurement temperature *n* is shown in parentheses following the species name, nd, no data. Note that estimates of $R_d$ result from the regression of *A* to irradiance above 20 μmol m$^{-2}$ s$^{-1}$, an irradiance higher than the Kok kink.

($F_{5,100}$ = 3.8, $P$ < 0.005) but not θ ($F_{5,100}$ = 1.5, $P$ = 0.19) or $R_d$ ($F_{5,100}$ = 1.5, $P$ = 0.19). Leaf absorptance varied significantly between species ($F_{5,198}$ = 203, $P$ < 0.001) ranging from 0.80 ± 0.006 (SEM) in *C. aquatilis* to 0.96 ± 0.002 in *P. frigidus* (Fig. 3). The six species mean α was 0.88 ± 0.03 (SEM, $n$ = 6 species).

## Comparison of measurements with terrestrial biosphere model parameterisation

The TBM $\phi_{CO_2.a}$ at 25°C ranges from 0.032 mol $CO_2$ mol$^{-1}$ absorbed quanta (LM3) to 0.060 mol $CO_2$ mol$^{-1}$ absorbed quanta (CLM4.5, Table 1 and Fig. 4). This variation in $\phi_{CO_2.a}$

largely reflects the variation in the model assumption of the fraction of light not used for photosynthesis ($f$, Table 1) with the exception of ED2, which has a notably lower absorptance in comparison with the other models (Table 1). Fig. 4 shows the effect of temperature on TBM $\phi_{CO_2.a}$ modeled for our measurement conditions. The TBM $\phi_{CO_2.a}$ decreases from 5°C to 25°C due to the effects of temperature on $\Gamma^*$ (Eqn 7) which reflects both the decreasing solubility of $CO_2$ and affinity of Rubisco for $CO_2$ relative to $O_2$ as temperature increases. The boxes in Fig. 4 show the combined dataset of $\phi_{CO_2.a}$ for all species measured at each temperature, including the limited number of measurements we were able to make at 25°C. We found a significant effect of temperature on $\phi_{CO_2.a}$ ($F_{2,122} = 44$, $P < 0.001$). The mean $\phi_{CO_2.a}$ measured at 5°C ($0.025 \pm 0.001$ SEM mol $CO_2$ mol$^{-1}$ absorbed quanta, $n = 50$ measurements) and 15°C ($0.037 \pm 0.001$ SEM mol $CO_2$ mol$^{-1}$ absorbed quanta, $n = 62$ measurements) were 45% and 18% lower than the mean $\phi_{CO_2.a}$ measured at 25°C ($0.045 \pm 0.003$ SEM mol $CO_2$ mol$^{-1}$ absorbed quanta, $n = 13$ measurements). The comparison of TBM and measured $\phi_{CO_2.a}$ showed that the mean model estimate of $\phi_{CO_2.a}$ at 25°C ($0.044 \pm 0.003$ SEM mol $CO_2$ mol$^{-1}$ absorbed quanta) was not significantly different from observations ($t_{(9)} = 0.26$, $P = 0.8$). However, below 25°C model assumptions and measured $\phi_{CO_2.a}$ diverge. At 15°C the measured mean $\phi_{CO_2.a}$ was 35% lower ($t_{(9)} = 4.8$, $P < 0.001$) than the TBM mean ($0.057 \pm 0.004$ SEM mols $CO_2$ mol$^{-1}$ absorbed quanta) and at 5°C the measured mean $\phi_{CO_2.a}$ was 60% lower ($t_{(9)} = 8.7$, $P < 0.001$) than the TBM mean ($0.063 \pm 0.004$ SEM mols $CO_2$ mol$^{-1}$ absorbed quanta, $n = 9$ models).

When combining data from all species, and including the limited data collected at 25°C, we observed a significant decrease in θ with decreasing temperature ($F_{2,122} = 5.8$, $P < 0.005$, Fig. 5). The TBMs that adopt the formulation for electron transport described by Eqn 4 (Farquhar & Wong, 1984) assume that $\theta = 0.7$ (solid line Fig. 5). Our data show that, at 25°C, this is a reasonable assumption (mean θ at 25°C $= 0.65 \pm 0.03$ SEM, $n = 13$ measurements, one sample $t_{(1)} = 1.5$, $P > 0.05$), but at 15°C mean θ was 29% lower than the model assumption ($0.50 \pm 0.03$ SEM, $n = 62$ measurements, one sample $t_{(1)} = 7.8$, $P < 0.001$) and at 5°C was 38% lower ($0.44 \pm 0.03$ SEM, $n = 50$ measurements, one sample $t_{(1)} = 8.1$, $P < 0.001$).

## Implications for modeled leaf-level $CO_2$ assimilation

To visualise the effect of the observed reductions in $\phi_{CO_2.i}$ and θ at low temperature we modeled leaf-level photosynthesis using the equations of FvCB, where $J$ was estimated using Eqn 4., together with our measured α (Fig. 3) and the parameterisation

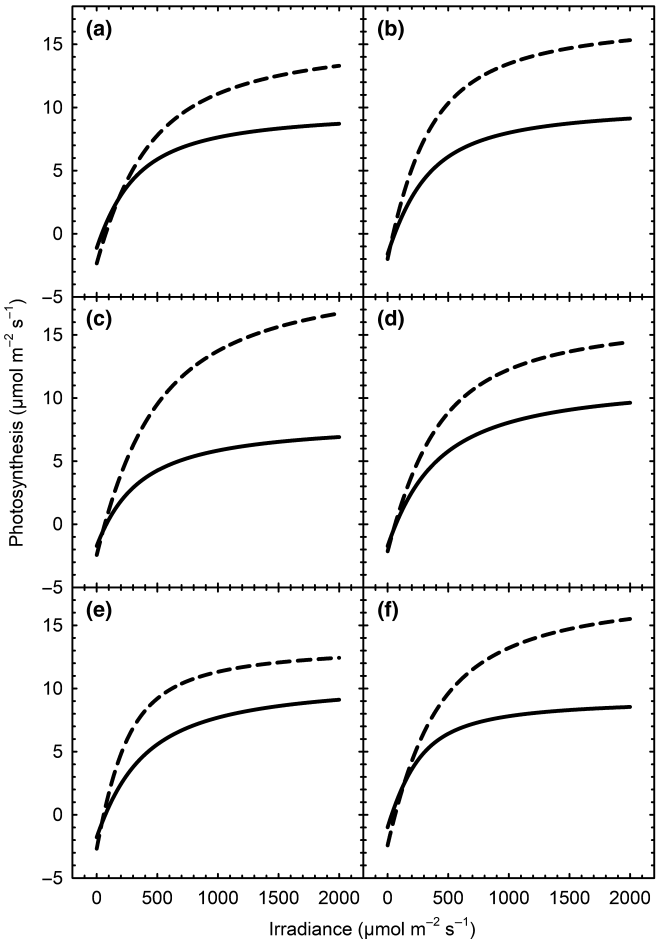


**Fig. 2** Synthetic light-response curves at *c.* 5°C (solid lines) and 15°C (broken lines) for *Arctagrostis latifolia* (a), *Arctophila fulva* (b), *Carex aquatilis* (c), *Eriophorum angustifolium* (d), *Petasites frigidus* (e) and *Salix pulchra* (f). Light-response curves were generated using Eqn 6 and the derived parameters presented in Table 2. The response of photosynthesis to irradiance measured at 25°C is not shown for individual species due to insufficient replication.

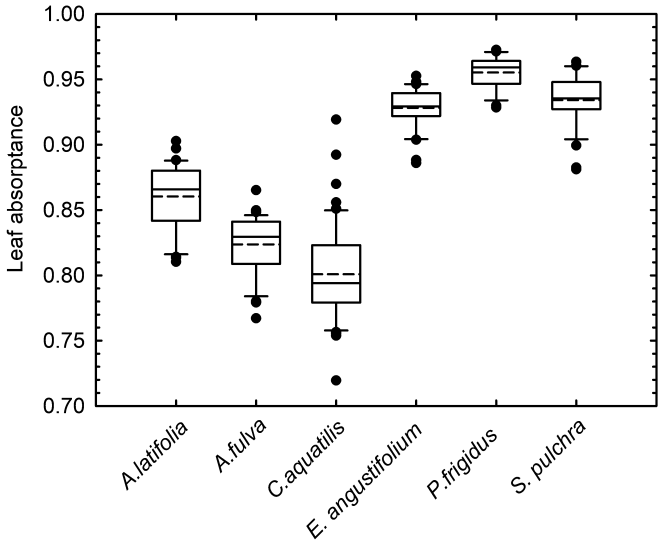


**Fig. 3** Tukey box plots showing the leaf absorptance of the six Arctic species studied in this investigation. Box plots show the interquartile range (box), median (solid line) and mean (broken line). The whiskers show the lowest and highest datum still within 1.5× interquartile range of the lower and upper quartiles. Outliers are shown as black circles (*Arctagrostis latifolia* $n = 37$, *Arctophila fulva* $n = 38$, *Carex aquatilis* $n = 52$, *Eriophorum angustifolium* $n = 41$, *Petasites frigidus* $n = 28$, *Salix pulchra* $n = 32$).

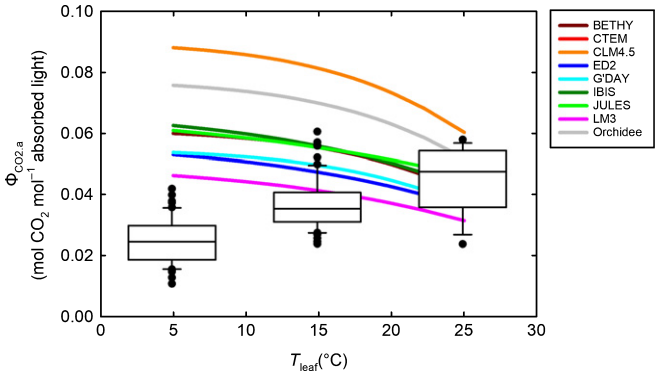


**Fig. 4** Tukey box plots showing the quantum yield of $CO_2$ fixation on an absorbed light basis ($\phi_{CO_2.a}$) for all measurements made at 5°C ($n = 50$), 15°C ($n = 63$) and 25°C ($n = 13$). Boxes show the interquartile range and median (solid line). The whiskers show lowest and highest datum still within 1.5× interquartile range of the lower and upper quartiles. Outliers are shown as black circles. The lines behind the box plots show the $\phi_{CO_2.a}$ for terrestrial biosphere models (TBMs) calculated using Eqns 7–10, the model specific parameterisation in Table 1 and measured $C_i$.

and activation energies associated with $V_{c,max}$ and $J_{max}$ measured for these same species at our field site (Rogers *et al.*, 2017b). Fig. 6 shows $A$ modeled assuming that $\phi_{CO_2.i}$ and θ do not decrease at low temperature, the current assumption in TBMs (broken lines, Fig. 6), and when we account for observed reductions in $\phi_{CO_2.i}$ and θ at low temperature as observed in this study (solid lines, Fig. 6). Fig. 6(c) shows that at 25°C model assumptions closely match observations but that as temperature is reduced to 15°C (Fig. 6b) and further to 5°C (Fig. 6a) the TBM assumptions result in a marked overestimation of $A$ at subsaturating irradiance. At an irradiance of 400 μmol $m^{-2}$ $s^{-1}$ TBMs with a fixed ϕ and θ over estimate leaf level $A$ by 1% at 25°C, 25% at 15°C and by 45% at 5°C (Fig. 6).

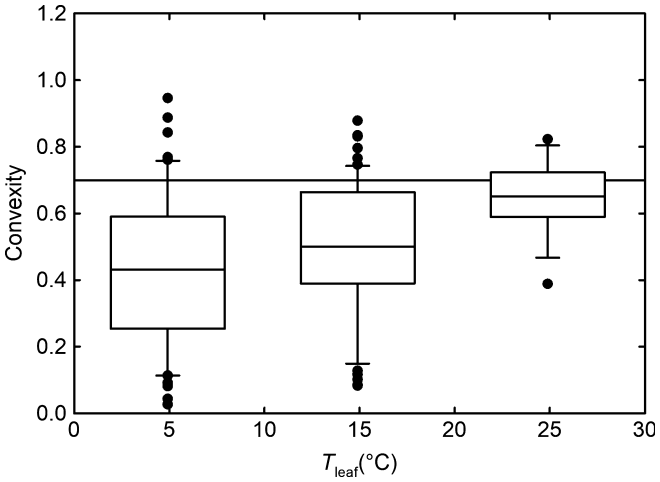


**Fig. 5** Tukey box plots showing the measured convexity of the response of photosynthesis to irradiance for all measurements made at 5°C, 15°C and 25°C. Boxes show the interquartile range and median (solid line). The whiskers show lowest and highest datum still within a 1.5× interquartile range of the lower and upper quartiles. Outliers are shown as black circles (5°C $n = 52$, 15°C $n = 67$, 25°C $n = 14$). The solid horizontal line indicates the model assumption of 0.7 (Farquhar & Wong, 1984).

Fig. 7 shows the normalised frequency of solar irradiance and mean daily air temperature during the thaw season at four eddy covariance sites located on the north slope of Alaska. The mean daily air temperatures for these four tundra sites were all below 10°C and irradiance was typically low (< 500 μmol $m^{-2}$ $s^{-1}$). Although these sites are typified by cold temperatures and low irradiance they also regularly experience periods of high light (for example Barrow; Fig. 1). Using Eqns 1–4 it is possible to model the utilisation of incident quanta by the Calvin cycle and the photorespiratory pathway (Long *et al.*, 1994). Fig. 8 shows the amount of light absorbed and utilised at 5°C, 15°C, and 25°C for a typical Arctic plant (we used the average α, $\phi_{ET.i}$ and θ determined in this study). Fig. 8 clearly demonstrates that these Arctic plants, like all plants, experience excess irradiance on a daily basis. At a typical moderate irradiance of 500 μmol quanta $m^{-2}$ $s^{-1}$, plants growing at 5°C can utilise 15% of incident irradiance for photosynthesis whereas plants growing at 15 and 25°C can utilise 26% and 44% of incident light respectively. At high irradiance (1500 μmol quanta $m^{-2}$ $s^{-1}$) the amount of light utilised increased only slightly but the percent of the incident irradiance that is now in excess of requirements for photosynthesis is 92%, 86% and 75% for plants growing at 5°C, 15°C and 25°C, respectively.

## Discussion

We have increased understanding of the response of photosynthesis to irradiance at low temperatures in Arctic species and demonstrated that, despite adaptation to a low growth temperature, reductions in ϕ and θ are readily observed at the low temperatures commonly experienced by Arctic vegetation. Our analysis shows that TBM parameterisation of ϕ and θ provides an accurate simulation of $CO_2$ assimilation at 25°C, the commonly used reference temperature for temperature-mediated processes in models (Rogers *et al.*, 2017a). However, because current TBM representation of ϕ and θ is insensitive to decreasing temperature, overestimation of these parameters at low temperature in TBMs has the potential for a marked overestimation of $CO_2$ assimilation at subsaturating irradiance across the high Arctic.

The significant species effect and interaction between species and temperature (5°C and 25°C) for $\phi_{CO_2.i}$ suggests a differential response to low temperatures among these species (Table 2). When considering this observation, in conjunction with the limited data collected at 25°C, it suggests that the temperature sensitivities of $\phi_{CO_2.i}$ to low temperature are different among species. For example the $\phi_{CO_2.i}$ in *P. frigidus* drops 4% between 25°C (0.053) and 15°C (0.051) but then 44% between 15°C and 5°C (0.028), whereas in *C. aquatilis* $\phi_{CO_2.i}$ drops 22% between 25°C (0.050) and 15°C (0.039) and then 38% between 15°C and 5°C (0.024). This implies that $\phi_{CO_2.i}$ in *C. aquatilis* shows a greater sensitivity to reductions in temperature than *P. frigidus*. Leaf absorptance varied significantly among species (0.80–0.96; Fig. 3) but on average was close to model assumptions (0.73–0.88, Table 1), suggesting that TBMs using a value close to 0.88 (the six species mean) are accurately parameterizing leaf absorptance in the Arctic PFT.

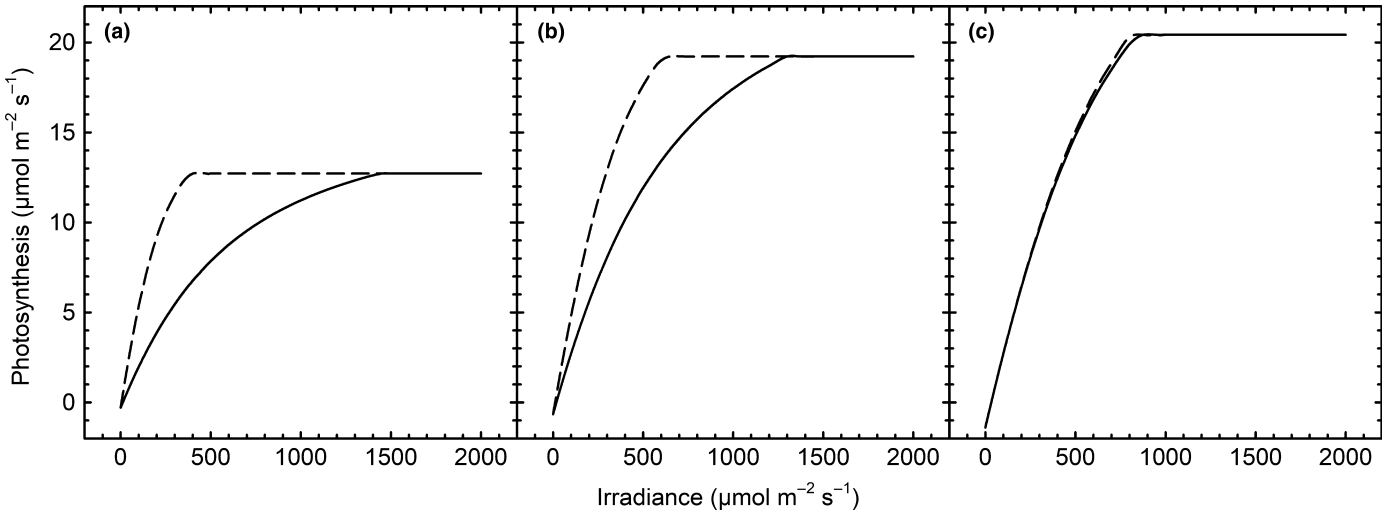


**Fig. 6** The response of photosynthesis to irradiance at 5°C (a), 15°C (b) and 25°C (c). Photosynthesis was modeled using the Eqns 1–7. The model was parameterised based on previous work on these Arctic species (Rogers *et al.*, 2017b). The solid lines show photosynthesis modeled using the mean absorptance (α, 0.88), quantum yield of $CO_2$ assimilation of incident irradiance ($\phi_{CO_2.i}$, 5°C, 0.028; 15°C, 0.042; 25°C, 0.051) and convexity (θ, 5°C, 0.44; 15°C, 0.5; 25°C, 0.65) observed in this study. The broken lines show photosynthesis modeled using the mean terrestrial biosphere model (TBM) assumption for α (0.84), the fraction of light absorbed by photosystem II that is not used for photochemistry (*f*, 0.37) and θ (0.7), where *f* and θ do not decrease at low temperature.

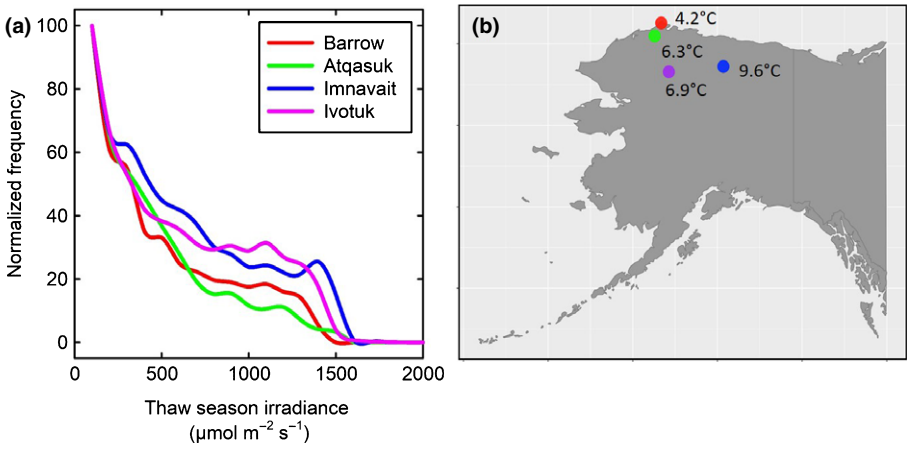


**Fig. 7** Normalised frequency distribution (arbitrary scale) of half hourly irradiance (a) and the mean daily air temperature during the thaw season (b). Data were retrieved from four Arctic tundra Ameriflux sites; Barrow, latitude 71.3225, longitude −156.6259, elevation 1 m, Atqasuk, latitude 70.4696, longitude −157.4089, elevation 15 m, the Imnavait creek watershed, latitude 68.6058, longitude −149.3110; elevation 920 m, and Ivotuk, latitude 68.4865, longitude −155.7503, elevation 568 m (Bret-Harte *et al.*, 2016; Oechel & Zona, 2016a,b,c). Thaw season is defined as commencing on the first day of the first three consecutive days in the calendar year with average temperature above freezing, and ending on the first day of the subsequent occurrence of 3 d with average temperatures below freezing. For a given site, data were taken from the most recent year available with complete or near complete data coverage during the thaw season period. Irradiance frequency is calculated using a bin size of 100 μmol m$^{-2}$ s$^{-1}$ for all data in which irradiance > 50 μmol m$^{-2}$ s$^{-1}$.

The $\phi_{CO_2}$ is known to be highly conserved in unstressed plants (Ehleringer & Bjorkman, 1977; Osborne & Garrett, 1983; Long *et al.*, 1993). Our estimate of $\phi_{CO_2.a}$ (0.045) at 25°C is lower than these upper estimates in the literature. For example, the high $\phi_{CO_2.a}$ measured by Long *et al.* (1993) when converted to our photorespiratory measurement conditions using Eqn 7 is 0.075. However, this may reflect the growth and measurement conditions of the plants. Many studies reporting high $\phi_{CO_2}$ are from healthy, unstressed plants that were often dark adapted before measurement or grown or measured at low irradiance (Long *et al.*, 1993; Singsaas *et al.*, 2001; Kromdijk *et al.*, 2016). Singsaas *et al.* (2001) surveyed measurements of $\phi_{CO_2}$ from the literature and reported that field-measured $\phi_{CO_2}$ values were consistently lower ($0.049 \pm 0.01$ SD) than these high estimates from unstressed plants. This finding suggests that the realised $\phi_{CO_2}$ in the field may be subject to reductions from maximum $\phi_{CO_2}$ due to photodamage and photoprotection mechanisms that are likely to occur under field conditions. Our estimate for $\phi_{CO_2.a}$ (0.045)

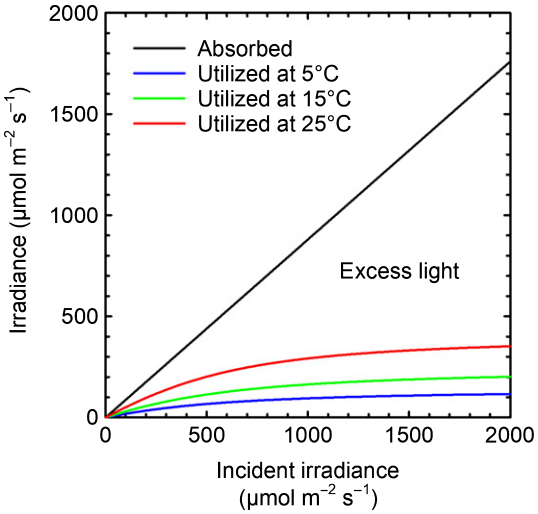


**Fig. 8** Modeled absorption (black line) and utilisation (colored lines) of incident irradiance by photosynthesis at 5°C (blue), 15°C (green), and 25°C (red). Utilised light was calculated assuming whole chain electron transport and a ratio of 2 quanta per electron (von Caemmerer, 2000) calculated using Eqns 1–4 as described previously (Long *et al.*, 1994). Temperature-specific parameterisation of convexity (θ), and the quantum yield of $CO_2$ assimilation of incident irradiance ($\phi_{CO_2.i}$), and absorptance (α) were taken from Table 2.

is comparable with the mean value of the TBMs evaluated here (0.044) suggesting that models are, on average, using estimates of ϕ that reflect the realised $\phi_{CO_2}$ observed under field conditions, but note the wide range of TBM parameterisation (Fig. 4).

Our observations of a reduction in $\phi_{CO_2.a}$ and θ with decreasing temperature in Arctic plants are consistent with observations from plants measured in temperate systems in which reductions in $\phi_{CO_2.a}$ and θ were also observed when plants experienced low temperatures (Bongi & Long, 1987; Groom *et al.*, 1991; Groom & Baker, 1992; Ogren & Evans, 1992; Long *et al.*, 1994). At high latitudes $\phi_{PSII}$ was shown to increase with winter warming of evergreen sub-Arctic shrubs in northern Sweden (Bokhorst *et al.*, 2010); this result is consistent with our observations of reduced $\phi_{CO_2}$ at low temperature. These, and other studies (Marchand *et al.*, 2006; Albert *et al.*, 2012) that measured $\phi_{PSII}$ in Arctic and sub-Arctic species, have also shown a range of $\phi_{PSII}$ (0.55–0.75) that is consistent with stressed vegetation, which is in contrast with the higher (0.83) and remarkably consistent $\phi_{PSII}$ of unstressed leaves (Baker, 2008). In Arctic shrubs, including *S. pulchra*, high xanthophyll pigment pools and high de-epoxidation of those pools support the potential for high xanthophyll cycle activity, and the deployment of photoprotective mechanisms in Arctic species that are consistent with acclimation or adaptation to stress (Magney *et al.*, 2017).

The irradiance and temperature conditions required to induce photoprotection, or cause photodamage in plants is complex, as are the conditions determining the dynamics and magnitude of the recovery process. Both induction and recovery are dependent upon a myriad of additional factors, for example leaf angle, leaf orientation, leaf canopy position, the proportion of direct and diffuse irradiance, the recent irradiance and temperature to which the plants have acclimated, season and leaf age (Bongi & Long, 1987; Long *et al.*, 1994; Garbulsky *et al.*, 2011; Williams *et al.*, 2014; Wong & Gamon, 2015a,b; Slattery *et al.*, 2018). The dynamics of recovery are highly variable, ranging from rapid (min to h) recovery from photoprotection or prolonged (days) depression of photosynthetic performance following severe photodamage (Bolharnordenkampf *et al.*, 1991; Farage & Long, 1991; Groom & Baker, 1992; Ogren & Evans, 1992; Long *et al.*, 1994; Zhu *et al.*, 2004; Takahashi & Murata, 2008; Kromdijk *et al.*, 2016; Slattery *et al.*, 2018). An important next step for field research will be to determine the dynamics of induction and recovery of photoprotection and photodamage in Arctic biomes. Remote sensing offers one approach that could be used to advance understanding of the dynamics of photoprotection through quantification of xanthophyll cycle pool sizes and de-epoxidation state (Gamon, 2015).

All the TBMs considered here assume constant values for ϕ and θ that are also identical for all PFTs. If the reductions in ϕ and θ observed at low temperature in this study are a pan-Arctic phenomenon, the typically subsaturating irradiance (Fig. 7a), in combination with regular episodes of saturating irradiance (Fig. 1), and the low mean daily air temperatures (Fig. 7b), suggest that current TBMs will have the potential to overestimate *A*. Previous theoretical analysis has shown that slow reversibility of NPQ at low temperature could reduce carbon gain by >30% in crop canopies (Zhu *et al.*, 2004) and suggests that ignoring the effects of photochemical protection and photodamage in Arctic PFTs could lead to a potentially large overestimation of carbon uptake at high latitudes. It is important to note that our modeling exercise is limited to a leaf-level assessment, with a single formulation of the many possible variants of the FvCB model of photosynthesis currently implemented in TBMs. Furthermore, the current parameterisation of TBMs, notably the widespread use of low values for $V_{c,max}$ (Rogers *et al.*, 2017b), would mask the overestimation of *A* at low temperature and low irradiance resulting from not including low temperature sensitivity of ϕ and θ. In this case, TBMs might get the right answer for the wrong reasons.

Given that leaf-level physiology is critical for robust projection of the response of the terrestrial biosphere to a changing climate, particularly rising [$CO_2$], it is essential that leaf physiology is represented accurately. We encourage the modeling community to further explore the impact of low temperature reductions on ϕ and θ in models with realistic parameterisation of Arctic vegetation derived from available data (Rogers *et al.*, 2017b), trait-environment correlation (Ali *et al.*, 2015) or optimisation theory (Smith *et al.* 2019), and an updated understanding of thermal acclimation (Kumarathunge *et al.*, 2019).

Our work clearly demonstrates that low temperature photoprotection or photodamage in Arctic vegetation is readily observed. These findings contradict the assumptions made by current models (Dietze, 2014). However, a further understanding of the conditions under which reductions in ϕ and θ can occur is required to fully understand the implications of a reduced ϕ and θ for the Arctic carbon cycle, and to enable confident implementation of this phenomenon in TBMs. As high latitude ecosystems warm rapidly over the next 50 yr (USGCRP, 2017), leaf-level photosynthesis will increase due to the strong temperature

dependency of photosynthesis. Our data suggest that the amelioration of the temperature-dependent reduction in ϕ and θ resulting from warmer growth temperatures may also contribute to anticipated increases in carbon gain in the Arctic as the climate warms.

## Acknowledgements

This work was supported by the Next-Generation Ecosystem Experiments (NGEE Arctic) project, which is supported by the Office of Biological and Environmental Research in the Department of Energy, Office of Science, and through the United States Department of Energy contract no. DE-SC0012704 to Brookhaven National Laboratory. Authors are grateful to Ukpeaġvik Iñupiat Corporation Science for logistical support.

## Author contributions

All authors collected data, AR, KSE and SPS analysed the data, AR wrote the first draft of the manuscript, KSE, SPS, and SDW contributed to the final version.

## ORCID

Kim S. Ely https://orcid.org/0000-0002-3915-001X
Alistair Rogers https://orcid.org/0000-0001-9262-7430
Shawn P. Serbin https://orcid.org/0000-0003-4136-8971
Stan D. Wullschleger https://orcid.org/0000-0002-9869-0446

## References

**Ainsworth EA, Rogers A. 2007.** The response of photosynthesis and stomatal conductance to rising $CO_2$: mechanisms and environmental interactions. *Plant, Cell & Environment* **30**: 258–270.

**Albert KR, Mikkelsen TN, Ro-Poulsen H, Arndal MF, Boesgaard K, Michelsen A, Bruhn D, Schmidt NM. 2012.** Solar UV-B effects on PSII performance in *Betula nana* are influenced by PAR level and reduced by EDU: results of a 3-year experiment in the High Arctic. *Physiologia Plantarum* **145**: 485–500.

**Ali AA, Xu CG, Rogers A, McDowell NG, Medlyn BE, Fisher RA, Wullschleger SD, Reich PB, Vrugt JA, Bauerle WL *et al.* 2015.** Global-scale environmental control of plant photosynthetic capacity. *Ecological Applications* **25**: 2349–2365.

**Allakhverdiev SI, Murata N. 2004.** Environmental stress inhibits the synthesis *de novo* of proteins involved in the photodamage-repair cycle of Photosystem II in *Synechocystis* sp. PCC 6803. *Biochimica et Biophysica Acta-Bioenergetics* **1657**: 23–32.

**Alton PB. 2017.** Retrieval of seasonal Rubisco-limited photosynthetic capacity at global FLUXNET sites from hyperspectral satellite remote sensing: impact on carbon modelling. *Agricultural and Forest Meteorology* **232**: 74–88.

**Aro EM, Virgin I, Andersson B. 1993.** Photoinhibition of photosystem 2 – inactivation, protein damage and turnover. *Biochimica et Biophysica Acta* **1143**: 113–134.

**Baker NR. 2008.** Chlorophyll fluorescence: a probe of photosynthesis *in vivo*. *Annual Review of Plant Biology* **59**: 89–113.

**Barber J, Andersson B. 1992.** Too much of a good thing – light can be bad for photosynthesis. *Trends in Biochemical Sciences* **17**: 61–66.

**Benomar L, Lamhamedi MS, Pepin S, Rainville A, Lambert M-C, Margolis HA, Bousquet J, Beaulieu J. 2017.** Thermal acclimation of photosynthesis and respiration of southern and northern white spruce seed sources tested along a regional climatic gradient indicates limited potential to cope with temperature warming. *Annals of Botany* **121**: 443–457.

**Bernacchi CJ, Leakey ADB, Heady LE, Morgan PB, Dohleman FG, McGrath JM, Gillespie KM, Wittig VE, Rogers A, Long SP *et al.* 2006.** Hourly and seasonal variation in photosynthesis and stomatal conductance of soybean grown at future $CO_2$ and ozone concentrations for 3 years under fully open-air field conditions. *Plant, Cell & Environment* **29**: 2077–2090.

**Bilger W, Bjorkman O. 1991.** Temperature-dependence of violaxanthin de-epoxidation and non-photochemical fluorescence quenching in intact leaves of *Gossypium hirsutum* L. and *Malva parviflora* L. *Planta* **184**: 226–234.

**Bockheim JG, Everett LR, Hinkel KM, Nelson FE, Brown J. 1999.** Soil organic carbon storage and distribution in Arctic Tundra, Barrow, Alaska. *Soil Science Society of America Journal* **63**: 934–940.

**Bokhorst S, Bjerke JW, Davey MP, Taulavuori K, Taulavuori E, Laine K, Callaghan TV, Phoenix GK. 2010.** Impacts of extreme winter warming events on plant physiology in a sub-Arctic heath community. *Physiologia Plantarum* **140**: 128–140.

**Bolharnordenkampf HR, Hofer M, Lechner EG. 1991.** Analysis of light-induced reduction of the photochemical capacity in field-grown plants – evidence for photoinhibition. *Photosynthesis Research* **27**: 31–39.

**Bonan GB, Lawrence PJ, Oleson KW, Levis S, Jung M, Reichstein M, Lawrence DM, Swenson SC. 2011.** Improving canopy processes in the Community Land Model version 4 (CLM4) using global flux fields empirically inferred from FLUXNET data. *Journal of Geophysical Research-Biogeosciences* **116**: G02014.

**Bongi G, Long SP. 1987.** Light-dependent damage to photosynthesis in olive leaves during chilling and high-temperature stress. *Plant, Cell & Environment* **10**: 241–249.

**Booth BBB, Jones CD, Collins M, Totterdell IJ, Cox PM, Sitch S, Huntingford C, Betts RA, Harris GR, Lloyd J. 2012.** High sensitivity of future global warming to land carbon cycle processes. *Environmental Research Letters* **7**. doi:10.1088/1748-9326/7/2/024002

**Bret-Harte S, Euskirchen E, Shaver G. 2016.** AmeriFlux US-ICs Imnavait Creek Watershed Wet Sedge Tundra. doi:10.17190/AMF/1246130

**Brown J, Everett KR, Webber PJ, MacLean SF, Murray DF. 1980.** The coastal tundra at Barrow. In: Brown J, Miller PC, Tiezen LL, Bunnell FL, eds. *An Arctic ecosystem: the coastal tundra at Barrow, Alaska.* Stroudsburg, PA, USA: Dowden, Hutchinson & Ross, Inc., 571.

**Buckley TN, Vice H, Adams MA. 2017.** The Kok effect in *Vicia faba* cannot be explained solely by changes in chloroplastic $CO_2$ concentration. *New Phytologist* **216**: 1064–1071.

**Busch FA, Sage RF, Farquhar GD. 2018.** Plants increase $CO_2$ uptake by assimilating nitrogen via the photorespiratory pathway. *Nature Plants* **4**: 46–54.

**von Caemmerer S. 2000.** *Biochemical models of leaf photosynthesis.* Collingwood, Vic., Australia: CSIRO Publishing.

**Chapin FS, Bret-Harte MS, Hobbie SE, Zhong HL. 1996.** Plant functional types as predictors of transient responses of Arctic vegetation to global change. *Journal of Vegetation Science* **7**: 347–358.

**Collatz GJ, Ball JT, Grivet C, Berry JA. 1991.** Physiological and environmental-regulation of stomatal conductance, photosynthesis and transpiration – a model that includes a laminar boundary-layer. *Agricultural and Forest Meteorology* **54**: 107–136.

**Croft H, Chen JM, Luo X, Bartlett P, Chen B, Staebler RM. 2016.** Leaf chlorophyll content as a proxy for leaf photosynthetic capacity. *Global Change Biology.* **23**: 3513–3524.

**Dietze MC. 2014.** Gaps in knowledge and data driving uncertainty in models of photosynthesis. *Photosynthesis Research* **119**: 3–14.

**Dusenge ME, Duarte AG, Way DA. 2019.** Plant carbon metabolism and climate change: elevated $CO_2$ and temperature impacts on photosynthesis, photorespiration and respiration. *New Phytologist* **221**: 32–49.

**Ehleringer J, Bjorkman O. 1977.** Quantum yields for $CO_2$ uptake in $C_3$ and $C_4$ plants – dependence on temperature, $CO_2$ and $O_2$ concentration. *Plant Physiology* **59**: 86–90.

**Farage PK, Long SP. 1991.** The occurrence of photoinhibition in an over-wintering crop of oilseed rape (*Brassica napus*) and its correlation with changes in crop growth. *Planta* **185**: 279–286.

**Farquhar GD, Busch FA. 2017.** Changes in the chloroplastic $CO_2$ concentration explain much of the observed Kok effect: a model. *New Phytologist* **214**: 570–584.

**Farquhar GD, Caemmerer SV, Berry JA. 1980.** A biochemical model of photosynthetic $CO_2$ assimilation in leaves of $C_3$ species. *Planta* **149**: 78–90.

**Farquhar GD, Wong SC. 1984.** An empirical model of stomatal conductance. *Australian Journal of Plant Physiology* **11**: 191–209.

**Foley JA, Prentice IC, Ramankutty N, Levis S, Pollard D, Sitch S, Haxeltine A. 1996.** An integrated biosphere model of land surface processes, terrestrial carbon balance, and vegetation dynamics. *Global Biogeochemical Cycles* **10**: 603–628.

**Forkel M, Carvalhais N, Rodenbeck C, Keeling R, Heimann M, Thonicke K, Zaehle S, Reichstein M. 2016.** Enhanced seasonal $CO_2$ exchange caused by amplified plant productivity in northern ecosystems. *Science* **351**: 696–699.

**Friedlingstein P, Cox P, Betts R, Bopp L, Von Bloh W, Brovkin V, Cadule P, Doney S, Eby M, Fung I *et al.* 2006.** Climate-carbon cycle feedback analysis: results from the $C^4$MIP model intercomparison. *Journal of Climate* **19**: 3337–3353.

**Friedlingstein P, Meinshausen M, Arora VK, Jones CD, Anav A, Liddicoat SK, Knutti R. 2014.** Uncertainties in CMIP5 climate projections due to carbon cycle feedbacks. *Journal of Climate* **27**: 511–526.

**Gamon JA. 2015.** Reviews and Syntheses: optical sampling of the flux tower footprint. *Biogeosciences* **12**: 4509–4523.

**Garbulsky MF, Peñuelas J, Gamon J, Inoue Y, Filella I. 2011.** The photochemical reflectance index (PRI) and the remote sensing of leaf, canopy and ecosystem radiation use efficiencies: a review and meta-analysis. *Remote Sensing of Environment* **115**: 281–297.

**Graven HD, Keeling RF, Piper SC, Patra PK, Stephens BB, Wofsy SC, Welp LR, Sweeney C, Tans PP, Kelley JJ *et al.* 2013.** Enhanced seasonal exchange of $CO_2$ by northern ecosystems since 1960. *Science* **341**: 1085–1089.

**Groom QJ, Baker NR. 1992.** Analysis of light-induced depressions of photosynthesis in leaves of a wheat crop during the winter. *Plant Physiology* **100**: 1217–1223.

**Groom QJ, Baker NR, Long SP. 1991.** Photoinhibition of holly (*Ilex aquifolium*) in the field during the winter. *Physiologia Plantarum* **83**: 585–590.

**Harper AB, Cox PM, Friedlingstein P, Wiltshire AJ, Jones CD, Sitch S, Mercado LM, Groenendijk M, Robertson E, Kattge J *et al.* 2016.** Improved representation of plant functional types and physiology in the Joint UK Land Environment Simulator (JULES v4.2) using plant trait information. *Geoscientific Model Development* **9**: 2415–2440.

**Heskel MA, Bitterman D, Atkin OK, Turnbull MH, Griffin KL. 2014.** Seasonality of foliar respiration in two dominant plant species from the Arctic tundra: response to long-term warming and short-term temperature variability. *Functional Plant Biology* **41**: 287–300.

**Keeling CD, Chin JFS, Whorf TP. 1996.** Increased activity of northern vegetation inferred from atmospheric $CO_2$ measurements. *Nature* **382**: 146–149.

**Kirschbaum MUF, Farquhar GD. 1987.** Investigation of the $CO_2$ dependence of quantum yield and respiration in *Eucalyptus pauciflora*. *Plant Physiology.* **83**: 1032–1036.

**Kromdijk J, Glowacka K, Leonelli L, Gabilly ST, Iwai M, Niyogi KK, Long SP. 2016.** Improving photosynthesis and crop productivity by accelerating recovery from photoprotection. *Science* **354**: 857–861.

**Kumarathunge DP, Medlyn BE, Drake JE, Tjoelker MG, Aspinwall MJ, Battaglia M, Cano FJ, Kelsey CR, Cavaleri MA, Cernusak LA *et al.* 2019.** Acclimation and adaptation components of the temperature dependence of plant photosynthesis at the global scale. *New Phytologist* **222**: 768–784.

**Lebauer DS, Wang D, Richter KT, Davidson CC, Dietze MC. 2013.** Facilitating feedbacks between field measurements and ecosystem models. *Ecological Monographs* **83**: 133–154.

**Leverenz JW, Falk S, Pilstrom CM, Samuelsson G. 1990.** The effects of photoinhibition on the photosynthetic light-response curve of green plant cells (*Chlamydomonas reinhardtii*). *Planta* **182**: 161–168.

**Lewin K, McMahon A, Ely KS, Serbin SP, Rogers A. 2016.** Zero Power Warming (ZPW) Chamber Prototype Measurements, Barrow, Alaska, 2016. Next Generation Ecosystem Experiments Arctic Data Collection Carbon Dioxide Information Analysis Center, Oak Ridge National Laboratory, Oak Ridge, TN, USA.

**Long SP, Bernacchi CJ. 2003.** Gas exchange measurements, what can they tell us about the underlying limitations to photosynthesis? Procedures and sources of error. *Journal of Experimental Botany* **54**: 2393–2401.

**Long SP, Humphries S, Falkowski PG. 1994.** Photoinhibition of photosynthesis in nature. *Annual Review of Plant Physiology and Plant Molecular Biology* **45**: 633–662.

**Long SP, Postl WF, Bolharnordenkampf HR. 1993.** Quantum yields for uptake of carbon dioxide in C-3 vascular plants of contrasting habitats and taxonomic groupings. *Planta* **189**: 226–234.

**Magney TS, Logan BA, Reblin JS, Boelman NT, Eitel JUH, Greaves HE, Griffin KL, Prager CM, Vierling LA. 2017.** Xanthophyll cycle activity in two prominent Arctic shrub species. *Arctic AntArctic and Alpine Research* **49**: 277–289.

**Marchand FL, Verlinden M, Kockelbergh F, Graae BJ, Beyens L, Nijs I. 2006.** Disentangling effects of an experimentally imposed extreme temperature event and naturally associated desiccation on Arctic tundra. *Functional Ecology* **20**: 917–928.

**Medlyn BE, McMurtrie RE, Dewar RC, Jeffreys MP. 2000.** Soil processes dominate the long-term response of forest net primary productivity to increased temperature and atmospheric $CO_2$ concentration. *Canadian Journal of Forest Research-Revue Canadienne de Recherche Forestiere* **30**: 873–888.

**Medvigy D, Wofsy SC, Munger JW, Hollinger DY, Moorcroft PR. 2009.** Mechanistic scaling of ecosystem function and dynamics in space and time: Ecosystem Demography model version 2. *Journal of Geophysical Research-Biogeosciences* **114**: G01002.

**Melton JR, Arora VK. 2016.** Competition between plant functional types in the Canadian Terrestrial Ecosystem Model (CTEM) vol 2.0. *Geoscientific Model Development* **9**: 323–361.

**Murata N, Nishiyama Y. 2018.** ATP is a driving force in the repair of photosystem II during photoinhibition. *Plant, Cell & Environment* **41**: 285–299.

**Norby RJ, Gu LH, Haworth IC, Jensen AM, Turner BL, Walker AP, Warren JM, Weston DJ, Xu CG, Winter K. 2017.** Informing models through empirical relationships between foliar phosphorus, nitrogen and photosynthesis across diverse woody species in tropical forests of Panama. *New Phytologist* **215**: 1425–1437.

**Oechel WC, Zona D. 2016a.** AmeriFlux US-Atq Atqasuk. doi:10.17190/AMF/1246029

**Oechel WC, Zona D. 2016b.** AmeriFlux US-Brw Barrow. doi:10.17190/AMF/1246041.

**Oechel WC, Zona D. 2016c.** AmeriFlux US-Ivo Ivotuk. doi:10.17190/AMF/1246067.

**Ogren E, Evans JR. 1992.** Photoinhibition of photosynthesis *in situ* in 6 species of *Eucalyptus*. *Australian Journal of Plant Physiology* **19**: 223–232.

**Oleson KW, Lawrence DM, Bonan GB, Drewniak B, Huang M, Koven CD, Levis S, Li F, Riley WJ, Subin ZM *et al.* 2013.** *Technical description of version 4.5 of the Community Land Model (CLM).* Boulder, CO, USA: National Center for Atmospheric Research.

**Ort DR. 2001.** When there is too much light. *Plant Physiology* **125**: 29–32.

**Osborne BA, Garrett MK. 1983.** Quantum yields for $CO_2$ uptake in some diploid and tetraploid plant-species. *Plant, Cell & Environment* **6**: 135–144.

**Piao S, Liu Z, Wang Y, Ciais P, Yao Y, Peng S, Chevallier F, Friedlingstein P, Janssens IA, Peñuelas J *et al.* 2018.** On the causes of trends in the seasonal amplitude of atmospheric $CO_2$. *Global Change Biology* **24**: 608–616.

**Posada JM, Lechowicz MJ, Kitajima K. 2009.** Optimal photosynthetic use of light by tropical tree crowns achieved by adjustment of individual leaf angles and nitrogen content. *Annals of Botany* **103**: 795–805.

**Ricciuto D, Sargsyan K, Thornton P. 2018.** The impact of parametric uncertainties on biogeochemistry in the $E^3$SM Land Model. *Journal of Advances in Modeling Earth Systems* **10**: 297–319.

**Rogers A. 2014.** The use and misuse of Vc, max in Earth System Models. *Photosynthesis Research* **119**: 15–29.

**Rogers A, Ely KS, Serbin SP. 2019.** Leaf photosynthetic parameters: quantum yield, convexity, respiration, gross $CO_2$ assimilation rate and raw gas exchange data, Barrow, Alaska, 2016. *Next Generation Ecosystem Experiments Arctic Data Collection*. Oak Ridge National Laboratory, Oak Ridge, TN, USA. doi: 10.5440/1482338

**Rogers A, Medlyn BE, Dukes JS, Bonan G, von Caemmerer S, Dietze MC, Kattge J, Leakey ADB, Mercado LM, Niinemets U *et al.* 2017a.** A roadmap for improving the representation of photosynthesis in Earth system models. *New Phytologist* **213**: 22–42.

**Rogers A, Serbin SP, Ely KS, Sloan VL, Wullschleger SD. 2017b.** Terrestrial biosphere models underestimate photosynthetic capacity and $CO_2$ assimilation in the Arctic. *New Phytologist* **216**: 1090–1103.

**Sargsyan K, Safta C, Najm HN, Debusschere BJ, Ricciuto D, Thornton P. 2014.** Dimensionality reduction for complex models via Bayesian compressive sensing. *International Journal for Uncertainty Quantification* **4**: 63–93.

**Schedlbauer JL, Fetcher N, Hood K, Moody ML, Tang JW. 2018.** Effect of growth temperature on photosynthetic capacity and respiration in three ecotypes of *Eriophorum vaginatum*. *Ecology and Evolution* **8**: 3711–3725.

**Serbin SP. 2019.** NGEE Arctic Leaf Spectral Absorptance, Barrow, Alaska, 2014–2016. *Next Generation Ecosystem Experiments Arctic Data Collection*. Oak Ridge National Laboratory, Oak Ridge, TN, USA. doi: 10.5440/1482337.

**Serbin SP, Singh A, Desai AR, Dubois SG, Jablonsld AD, Kingdon CC, Kruger EL, Townsend PA. 2015.** Remotely estimating photosynthetic capacity, and its response to temperature, in vegetation canopies using imaging spectroscopy. *Remote Sensing of Environment* **167**: 78–87.

**Serbin SP, Singh A, McNeil BE, Kingdon CC, Townsend PA. 2014.** Spectroscopic determination of leaf morphological and biochemical traits for northern temperate and boreal tree species. *Ecological Applications* **24**: 1651–1669.

**Shaver GR, Chapin FS, Billings WD. 1979.** Ecotypic differentiation in *Carex aquatilis* on ice-wedge polygons in the Alaskan coastal tundra. *Journal of Ecology* **67**: 1025–1046.

**Shiklomanov AN, Dietze MC, Viskari T, Townsend PA, Serbin SP. 2016.** Quantifying the influences of spectral resolution on uncertainty in leaf trait estimates through a Bayesian approach to RTM inversion. *Remote Sensing of Environment* **183**: 226–238.

**Shiklomanov NI, Streletskiy DA, Nelson FE, Hollister RD, Romanovsky VE, Tweedie CE, Bockheim JG, Brown J. 2010.** Decadal variations of active-layer thickness in moisture-controlled landscapes, Barrow, Alaska. *Journal of Geophysical Research-Biogeosciences* **115**: G00104.

**Singsaas EL, Ort DR, DeLucia EH. 2001.** Variation in measured values of photosynthetic quantum yield in ecophysiological studies. *Oecologia* **128**: 15–23.

**Slattery RA, Walker BJ, Weber APM, Ort DR. 2018.** The impacts of fluctuating light on crop performance. *Plant Physiology* **176**: 990–1003.

**Smith NG, Dukes JS. 2013.** Plant respiration and photosynthesis in global-scale models: incorporating acclimation to temperature and $CO_2$. *Global Change Biology* **19**: 45–63.

**Smith NG, Keenan TF, Prentice IC, Wang H, Wright IJ, Niinemets U, Crous KY, Domingues TF, Guerrieri R, Ishida FY *et al.* 2019.** Global photosynthetic capacity is optimized to the environment. *Ecology Letters.* **22**: 506–517.

**Takahashi S, Murata N. 2008.** How do environmental stresses accelerate photoinhibition? *Trends in Plant Science* **13**: 178–182.

**Tcherkez G, Gauthier P, Buckley TN, Busch FA, Barbour MM, Bruhn D, Heskel MA, Gong XY, Crous KY, Griffin K *et al.* 2017.** Leaf day respiration: low $CO_2$ flux but high significance for metabolism and carbon balance. *New Phytologist* **216**: 986–1001.

**Thomas RT, Prentice LC, Graven H, Ciais P, Fisher JB, Hayes DJ, Huang MY, Huntzinger DN, Ito A, Jain A *et al.* 2016.** Increased light-use efficiency in northern terrestrial ecosystems indicated by $CO_2$ and greening observations. *Geophysical Research Letters* **43**: 11339–11349.

**USGCRP. 2017. Wuebbles DJ, Fahey DW, Hibbard KA, Dokken DJ, Stewart BC, Maycock TK, eds.** *Climate Science Special Report: Fourth National Climate Assessment*. Washington, DC, USA.

**Varhammar A, Wallin G, McLean CM, Dusenge ME, Medlyn BE, Hasper TB, Nsabimana D, Uddling J. 2015.** Photosynthetic temperature responses of tree species in Rwanda: evidence of pronounced negative effects of high temperature in montane rainforest climax species. *New Phytologist* **206**: 1000–1012.

**Walker AP, Beckerman AP, Gu LH, Kattge J, Cernusak LA, Domingues TF, Scales JC, Wohlfahrt G, Wullschleger SD, Woodward FI. 2014.** The relationship of leaf photosynthetic traits $V_{cmax}$ and $J_{max}$ to leaf nitrogen, leaf phosphorus, and specific leaf area: a meta-analysis and modeling study. *Ecology and Evolution* **4**: 3218–3235.

**van de Weg MJ, Shaver GR, Salmon VG. 2013.** Contrasting effects of long term versus short-term nitrogen addition on photosynthesis and respiration in the Arctic. *Plant Ecology* **214**: 1273–1286.

**Williams M, Rastetter EB, Van der Pol L, Shaver GR. 2014.** Arctic canopy photosynthetic efficiency enhanced under diffuse light, linked to a reduction in the fraction of the canopy in deep shade. *New Phytologist* **202**: 1266–1276.

**Wong CYS, Gamon JA. 2015a.** The photochemical reflectance index provides an optical indicator of spring photosynthetic activation in evergreen conifers. *New Phytologist* **206**: 196–208.

**Wong CYS, Gamon JA. 2015b.** Three causes of variation in the photochemical reflectance index (PRI) in evergreen conifers. *New Phytologist* **206**: 187–195.

**Wu J, Kobayashi H, Stark SC, Meng R, Guan KY, Tran NN, Gao SC, Yang W, Restrepo-Coupe N, Miura T *et al.* 2018.** Biological processes dominate seasonality of remotely sensed canopy greenness in an Amazon evergreen forest. *New Phytologist* **217**: 1507–1520.

**Yamori W, Hikosaka K, Way DA. 2014.** Temperature response of photosynthesis in $C_3$, $C_4$, and CAM plants: temperature acclimation and temperature adaptation. *Photosynthesis Research* **119**: 101–117.

**Yin X, Struik PC. 2009.** C-3 and C-4 photosynthesis models: an overview from the perspective of crop modelling. *Njas-Wageningen Journal of Life Sciences* **57**: 27–38.

**Zhu XG, Ort DR, Whitmarsh J, Long SP. 2004.** The slow reversibility of photosystem II thermal energy dissipation on transfer from high to low light may cause large losses in carbon gain by crop canopies: a theoretical analysis. *Journal of Experimental Botany* **55**: 1167–1175.

**Ziehn T, Kattge J, Knorr W, Scholze M. 2011.** Improving the predictability of global $CO_2$ assimilation rates under climate change. *Geophysical Research Letters* **38**: L10404.

## Supporting Information

Additional Supporting Information may be found online in the Supporting Information section at the end of the article.

**Fig. S1** Raw data associated with measurement of light-response curves in three individual leaves measured at three different temperatures.

Please note: Wiley Blackwell are not responsible for the content or functionality of any Supporting Information supplied by the authors. Any queries (other than missing material) should be directed to the *New Phytologist* Central Office.